Overview of Fundus Lesions Associated with Pathologic Myopia

2

Kyoko Ohno-Matsui

Abstract

Various kinds of lesions of myopic maculopathy occur in the posterior fundus of the eyes with pathologic myopia (PM), which could impair the vision. In addition to META-PM classification, the recent OCT-based classification clearly showed that the lesions of myopic maculopathy were characterized by "extreme thinning of the choroid," "macular Bruch's membrane defects," "macular retinoschisis and tractional lesions," and "dome-shaped macula." The underlying cause of developing these lesions is a deformity of the eye represented by posterior staphylomas. In this chapter, an overview of posterior staphyloma and each lesion of myopic maculopathy will be presented.

Keywords

Pathologic myopia · Posterior staphyloma · Myopic maculopathy · 3D MRI · Optical coherence tomography

2.1 Introduction

In eyes with pathologic myopia (PM), various kinds of lesions are present in different regions of the fundus, e.g., in the macula, mid-periphery, periphery, and on the optic disc (Fig. 2.1). The different kinds of lesions often coexist which makes an accurate diagnosis of each type of lesion difficult. In this Atlas, morphological features of each lesion associated with PM are presented based on recent multimodal imaging technology. First, an important cause of developing these lesions, posterior staphylomas, is described.

K. Ohno-Matsui (✉)
Department of Ophthalmology and Visual Science, Tokyo Medical and Dental University, Tokyo, Japan
e-mail: k.ohno.oph@tmd.ac.jp

2.2 Posterior Staphylomas: A Cause of Developing Myopic Maculopathy

A posterior staphyloma is a posterior outpouching of the posterior segment of the eye (Fig. 2.2). Posterior staphylomas are a hallmark of pathologic myopia and are one of the major causes of the development of myopic maculopathy [1–6].

In spite of its importance, there was no standardized definition of posterior staphylomas. Posterior staphylomas were occasionally confused with a simple backward bowing of the sclera which was commonly seen in the OCT images of highly myopic eyes.

Spaide [7] presented a comprehensive definition of posterior staphylomas in which he stated that a posterior staphyloma was an outpouching of a circumscribed region of the posterior pole of the eye that had a radius of curvature that was shorter than the radius of curvature of the adjacent eye wall (Fig. 2.3). The important point is that the formation of a staphyloma is an independent phenomenon that can develop from the continuous elongation of the axial length. Supporting this, staphylomas can also occur in non-axially elongated eyes [8] (Fig. 2.3d).

The importance of staphylomas is in its affected area of the eye. In the process of axial elongation, the equatorial region is mainly expanded while the posterior aspect of the eye is relatively unaffected (Fig. 2.3b). However, a staphyloma causes a deformity of the posterior pole of the eye where the visually important tissues, such as the macula and optic nerve head, are situated. It can easily be imagined that staphylomas can mechanically damage these tissues which can then lead to an impairment of vision. Supporting this, highly myopic eyes with staphylomas have poorer vision, and more commonly have myopic macular pathological lesions [2].

Curtin [9] examined staphylomas by ophthalmoscopic observations and chart drawings, and he classified them into 10 different types. Later, Ohno-Matsui [2] made a simpler

K. Ohno-Matsui (ed.), *Atlas of Pathologic Myopia*, https://doi.org/10.1007/978-981-15-4261-9_2

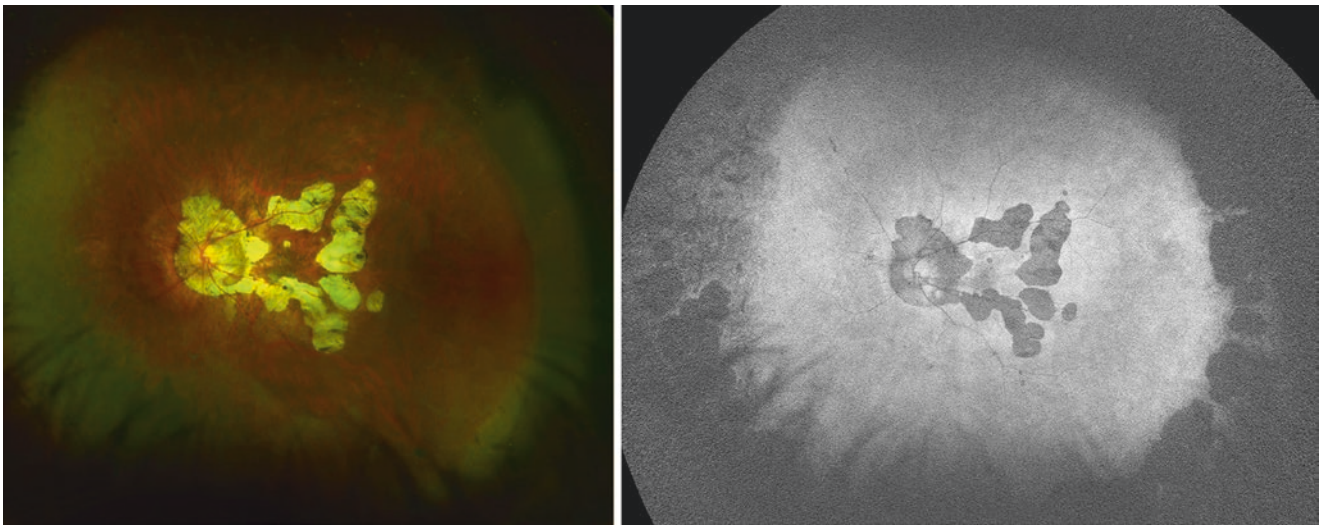

Fig. 2.1 Different types of fundus lesions can be seen in an eye with pathologic myopia in fundus photo (left) and in fundus autofluorescence image (right). Left fundus of a 67-year-old woman with an axial length of 34.9 mm. Ultra-widefield fundus image shows multiple lesions of patchy atrophy in and around the macula. A very large peripapillary atrophy is observed. Yellowish diffuse atrophy is seen around the peripapillary atrophy. Multiple cobblestone lesions are seen in the periphery

Fig. 2.2 Macroscopic images of staphylomas (modified with permission from the textbook *Pathologic Myopia*, Courtesy of Professor Emeritus Shigekuni Okisaka of the National Defense Medical College, Saitama, Japan). (left) A highly myopic eye with a narrow, macular staphyloma. The macular area is protruded posteriorly, and the sclera is extremely thinned in the protruded area. The axial length of the globe is 29 mm. (right) A highly myopic eye with large, multiple protrusions in a wide, macular staphyloma. Both, the peripapillary and macular regions, are protruded posteriorly. A large chorioretinal atrophy is seen extending over the entire posterior fundus. Axial length of the globe is 37 mm

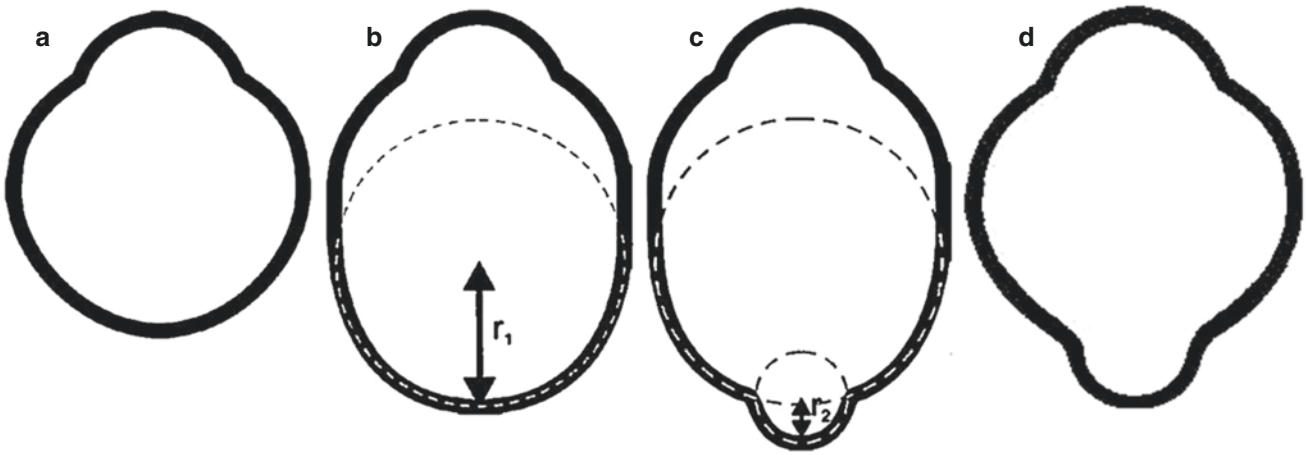

Fig. 2.3 Definition of posterior staphyloma (modified with permission from the Spaide [7]). (**a**) Emmetropic eye. (**b**) Axial myopia without posterior staphyloma. Axial elongation is present mainly in the equatorial region that does not induce an altered curvature in the posterior aspect of the eye. (**c**) A second curvature occurs in the posterior portion of the eye, and this second curvature has a shorter radius of curvature (r_2) than the surrounding eye wall (r_1). This secondary curve is a staphyloma. (**d**) In some eyes, a staphyloma characterized by a secondary curvature (r_2) can occur without marked axial elongation

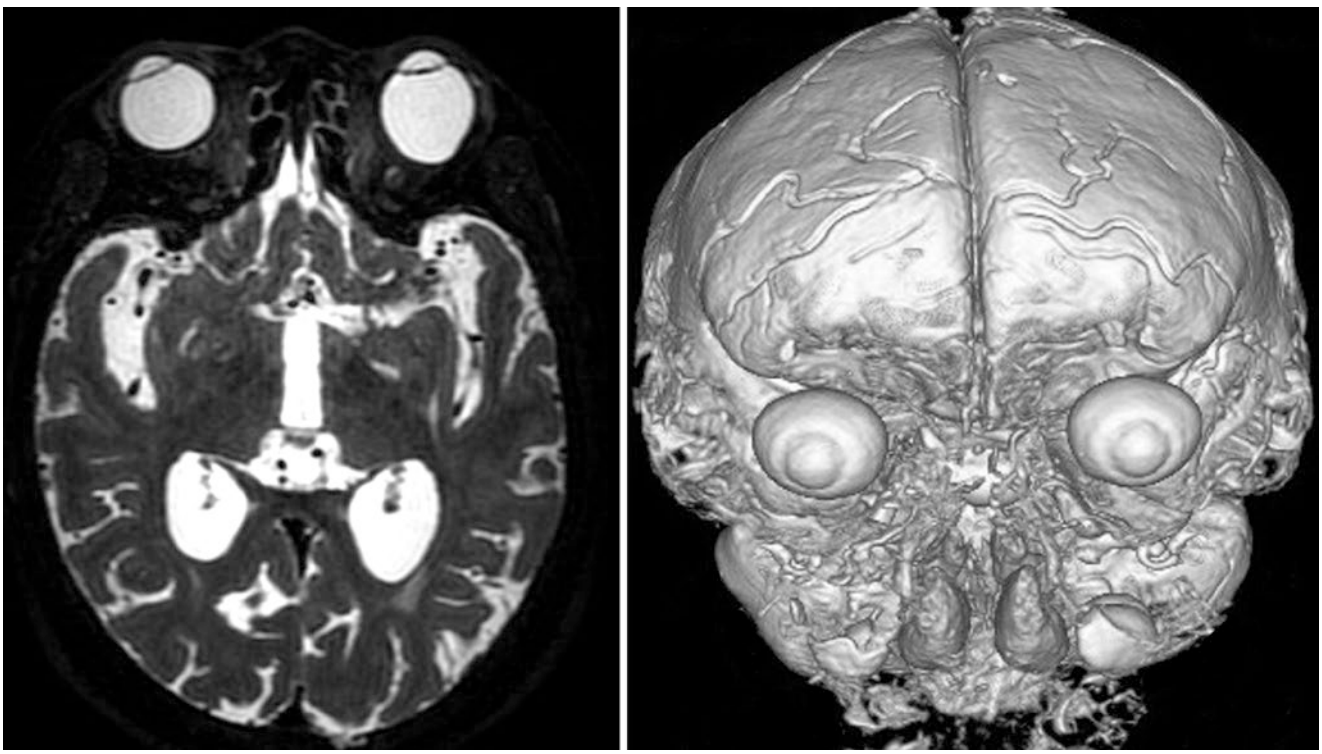

Fig. 2.4 Three-dimensional magnetic resonance imaging (3D MRI) of an eye. (left) 2D image of T2-weighed MRI shows unilateral high myopia. (right) Using volume rendering of T2-weighed MRI image, 3D view is created. Then the 3D image of the eye is extracted by trimming the surrounding tissue

classification and renamed staphylomas according to their size and location (see Chap. 3).

Most of the studies analyzing staphylomas used ophthalmoscopic observations and were subjective. Moriyama et al. [1] used modified 3D MRI technology to evaluate the entire shape of the eye (Fig. 2.4). This was a very powerful method, and it allowed them to classify the different shapes of eyes with staphylomas more extensively and accurately. However, 3D MRI is still not feasible as a screening technique. To overcome this deficit, we have turned to ultra-widefield OCT which had been recently introduced (Fig. 2.5) [10, 11]. The morphological shape of the staphylomas is clearly visible for their entire extent in the ultra-widefield OCT images. Different from 3D

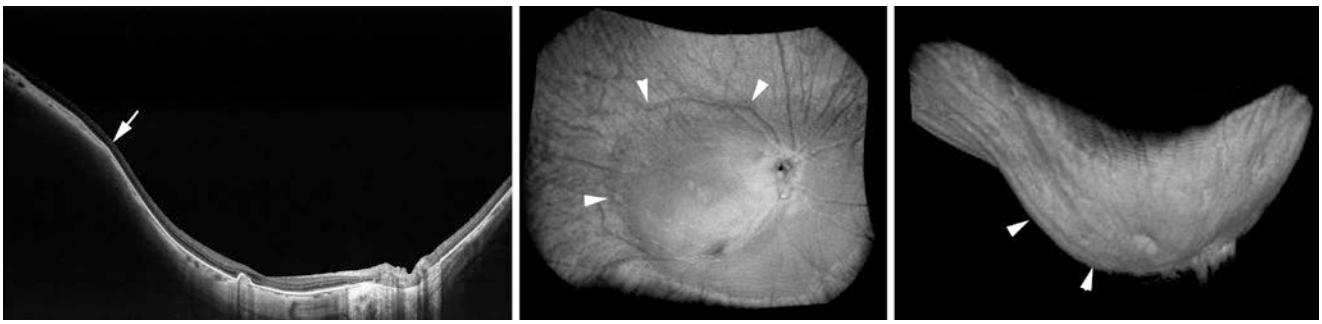

Fig. 2.5 Ultra-widefield OCT image of an eye with a posterior staphyloma. (left) B-scan shows a posterior displacement of the sclera in the area of a staphyloma. An arrow shows a staphyloma edge. (middle) 3D reconstructed image viewed from the front shows a staphyloma (outlined by arrowheads). (right) 3D reconstructed image viewed from the side shows a posterior protrusion due to staphyloma (arrowheads)

MRI, a detailed structure of the retina and the optic nerve are also visible, and these images show how eye deformities represented by staphylomas mechanically affect the visually important tissues.

Many of the fundus lesions associated with PM are difficult to cure; however, based on these imaging data, future treatments to prevent and treat staphylomas before blinding complications occur are expected.

2.3 Myopic Maculopathy: Diffuse Atrophy and Patchy Atrophy

In 2015, a consensus classification of myopic maculopathy was established based on fundus photographs by a group of retina experts. This group was named the Meta-analysis for Pathologic Myopia (META-PM) Study group [12]. In this META-PM classification, myopic maculopathy was classified into five categories; Category 0, "no maculopathy"; Category 1, "tessellated fundus"; Category 2, "diffuse choroidal atrophy"; Category 3, "patchy choroidal atrophy"; and Category 4, "macular atrophy." Three additional features to supplement these categories were defined as "plus" lesions; namely, lacquer cracks, myopic choroidal neovascularization (myopic CNV), and Fuchs' spot.

The META-PM classification is a well-established classification and has been widely used in many studies [5, 13, 14]. However, this classification is based on fundus photographs, and as is well known, the tone of the color of the fundus is affected by degree of fundus pigmentation which greatly differs among different ethnic groups. Thus, such photographical classification will depend on the ethnicity of the patient and will still be subjective. In addition, longitudinal studies with an 18 year follow-up period showed that most of the macular atrophy was CNV-related [5], i.e., the macular atrophy gradually developed around a CNV and did not develop without a preexisting myopic CNV. This indicated that a progression from Category 3 to Category 4 in the META-PM classification was very rare.

The imaging of the fundus of the eye has been greatly advanced especially for the OCT images. Earlier studies using enhanced depth imaging (EDI)-OCT and swept-source OCT showed a thinning of the choroid in myopic eyes [15, 16]. In eyes with PM, the choroid is extremely thin and is occasionally completely absent with large choroidal vessels remaining sporadically. Compared to retinal and scleral thinning, the choroidal thinning is disproportionately notable. Such extreme thinning of the choroid first develops temporal to the optic disc in childhood [17], and it expands and then involves the macular area. Choroidal thinning progresses from tessellation to diffuse choroidal atrophy [18]; however, no further thinning is noted from diffuse atrophy to patchy atrophy [18]. Recent swept-source OCT studies showed that patchy choroidal atrophies were not simply atrophic areas but were holes in Bruch's membrane (BM) [19]. These findings suggested a possibility that the lesions of myopic maculopathy can be categorized according to the degree and extent of the choroidal thinning as well as to the formation of BM holes [18].

Artificial intelligence (AI) is expected to become a powerful method to diagnose and evaluate the progression of myopic maculopathy. In addition, an OCT-based classification of myopic maculopathy is considered to best fit the AI diagnosis. Please see Chap. 4 for details of OCT-based classification (see Chap. 17).

2.4 Myopic Maculopathy; Myopic Macular Neovascularizations (MNV)

A myopic macular neovascularization (MNV) is also known as myopic CNV. However recent OCT studies revealed that at least some myopic CNVs were originated directly from intra-

scleral branches of short posterior ciliary arteries, myopic macular neovascularization (MNV) is considered a more accurate term. MNV is a major cause of a reduction of central vision in patients with PM, and it develops in 10% of highly myopic eyes [20]. When untreated, most of the patients with MNV have the best-corrected visual acuity (BCVA) of <0.1 at 5 years after the onset of the MNV [21]. The cause of a long-term vision reduction in eyes with PM is mainly due to the development of MNV-related macular atrophy rather than a recurrence or growth of the MNV [5, 6, 21].

A breakthrough in the prognosis of MNV was the application of anti-VEGF therapies [22–24]. The difference between anti-VEGF therapies and other therapies such as photodynamic therapy is that the former causes a marked shrinkage of the MNV. For small and non-subfoveal MNVs, it is quite common for them to completely disappear after the anti-VEGF therapy [25]. In the eyes whose MNV completely disappeared, the MNV-related macular atrophy, which is a long-term complication of MNV, does not develop. However, in the eyes whose MNV shrinks but does not disappear, MNV-related macular atrophy gradually develops and impairs the vision in the long-term. Swept-source OCT showed that the MNV-related macular atrophy was due to BM holes [26] similar to patchy atrophy, and thus it is different from the geographic atrophy present in age-related macular degeneration. To improve the long-term prognosis of MNV, it is necessary to prevent the formation and enlargement of BM holes around the MNV remnants.

In addition to the advancement of treatments, the improvements of imaging and diagnosing MNV have been made. The diagnosis of MNV was previously made with fundus observations and fluorescein angiograms. Besides OCT detection of MNVs, OCT angiography has been useful for detecting and analyzing vascular networks. However, a MNV is small and less active than the CNV associated with AMDs. It is sometimes difficult to obtain clear images with OCT angiography. Thus, for proper diagnosis of the presence and the activity of MNVs, multimodal imaging by OCT, OCT angiography, and fluorescein angiogram are recommended [25, 27, 28]. Functional analyses using fundus microperimetry, such as by MP3, are also useful.

2.5 Myopic Macular Retinoschisis and Tractional Lesions

The use of OCT has led to the identification of new pathologies associated with PM, e.g., myopic macular retinoschisis and dome-shaped macula (DSM). Takano and Kishi [29] first reported that patients with PM had macular retinoschisis before developing a macular hole retinal detachment. With the improved resolution of OCT instruments, other pathologies have been clarified, such as foveal retinal detachment, lamellar macular holes, retinal vascular microfolds, and paravascular lamellar holes [30–35]. Myopic macular retinoschisis was originally thought to always develop in eyes with a posterior staphyloma [29], but recent ultra-widefield OCT images showed that it was also present in eyes without a staphyloma [11]. Vitreous abnormalities in eyes with PM may play important roles in the development of myopic macular retinoschisis in eyes without an evident staphyloma [36, 37].

The usefulness of surgeries for myopic traction maculopathy is widely known [38, 39]. Modified surgical techniques such as fovea-sparing ILM peeling is now being widely used [40, 41]. The surgical indications for this procedure still need to be standardized. In addition, how the surgical outcome is quantified also needs to be determined. Besides the anatomical outcomes, functional outcomes by fundus microperimetry are recommended [42].

2.6 Dome-Shaped Macula (DSM)

A DSM is an inward protrusion of the macula area that can be identified by OCT [43, 44], and it is due to a local thickening of the sclera in the macular region [45]. The DSM is associated with various macular complications such as serous retinal detachment (RD) and MNV [46]. Although the mechanism(s) causing the formation of a DSM has not been definitively determined, the presence of macular BM defects may be one cause [47].

2.7 Conclusions

Various pathological lesions are present in wide areas of the fundus in eyes with PM, e.g., a peripheral avascular zone in 360 degrees [48], formation of a macular vortex vein [49], and radial tracts spreading from the staphyloma edge [50]. These pathological changes that develop in eyes with PM are probably related to the axial elongation and staphylomas present in eyes with PM.

The shape of the eye and ocular circulation, especially the choroidal circulation, are markedly altered in eyes with PM (Fig. 2.6, see Chap. 16) [49]. Such changes cause mechanical damage of the retina/choroid/sclera and the optic nerve. It is recommended that thorough examinations regarding a relationship between fundus pathologies and the eye shape should be conducted. It is important to clarify where the mechanical damage is loaded in the eyes with PM. Many pathologies in PM might be "mechanical."

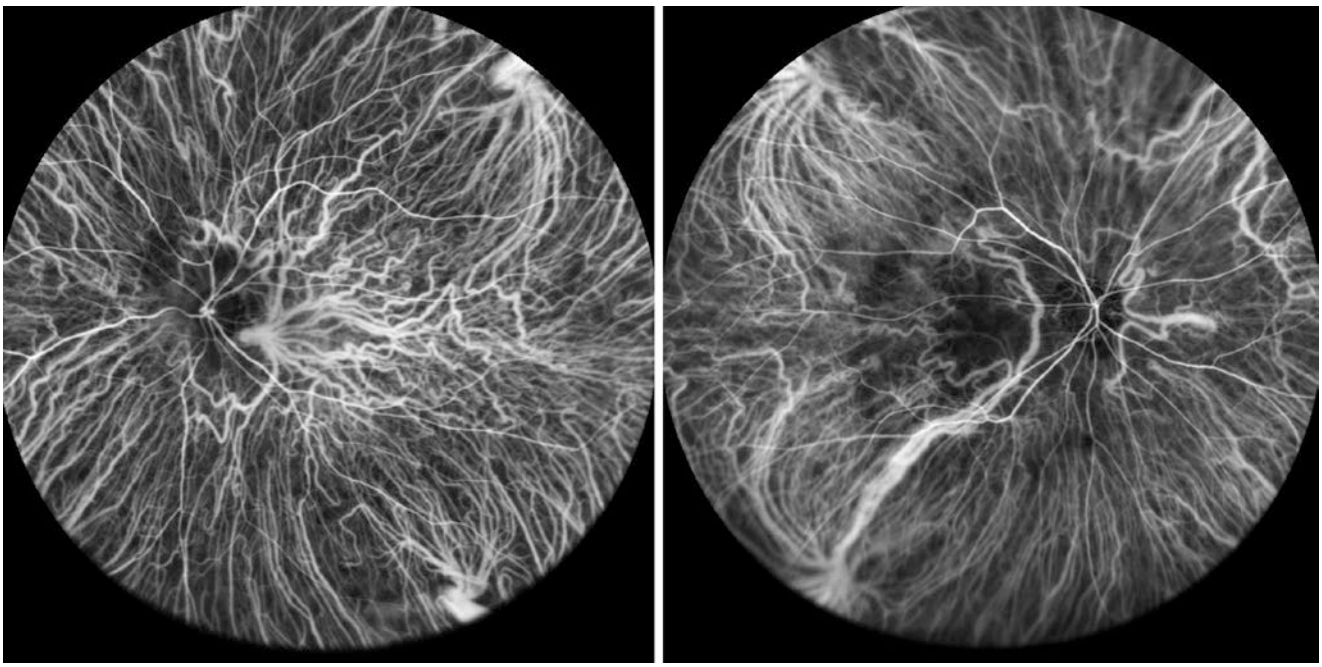

Fig. 2.6 Changes of choroidal vasculature shown by widefield indocyanine green angiography. (left) Macular vortex vein collects the choroidal venous blood and exits around the optic nerve after forming an ampulla. The choroidal venous flow is opposite within and outside the staphyloma. (right) Choroidal veins cannot go beyond the upper staphyloma edge and most of the macular choroidal venous blood drains to the lower temporal vortex vein through many collaterals

References

1. Moriyama M, Ohno-Matsui K, Hayashi K, et al. Topographical analyses of shape of eyes with pathologic myopia by high-resolution three dimensional magnetic resonance imaging. Ophthalmology. 2011;118(8):1626–37.
2. Ohno-Matsui K. Proposed classification of posterior staphylomas based on analyses of eye shape by three-dimensional magnetic resonance imaging. Ophthalmology. 2014;121(9):1798–809.
3. Vongphanit J, Mitchell P, Wang JJ. Prevalence and progression of myopic retinopathy in an older population. Ophthalmology. 2002;109(4):704–11.
4. Yan YN, Wang YX, Yang Y, et al. Ten-year progression of myopic maculopathy: The Beijing eye study 2001–2011. Ophthalmology. 2018;125:1253–63.
5. Fang Y, Yokoi T, Nagaoka N, et al. Progression of myopic maculopathy during 18-year follow-up. Ophthalmology. 2018;125(6):863–77.
6. Hayashi K, Ohno-Matsui K, Shimada N, et al. Long-term pattern of progression of myopic maculopathy: a natural history study. Ophthalmology. 2010;117(8):1595–611.
7. Spaide RF. Staphyloma: part 1. New York: Springer; 2013. p. 167–76.
8. Wang NK, Wu YM, Wang JP, et al. Clinical characteristics of posterior staphylomas in myopic eyes with axial length shorter than 26.5 mm. Am J Ophthalmol. 2016;162:180–90.
9. Curtin BJ. The posterior staphyloma of pathologic myopia. Trans Am Ophthalmol Soc. 1977;75:67–86.
10. Shinohara K, Shimada N, Moriyama M, et al. Posterior Staphylomas in pathologic myopia imaged by Widefield optical coherence tomography. Invest Ophthalmol Vis Sci. 2017;58(9):3750–8.
11. Shinohara K, Tanaka N, Jonas JB, et al. Ultra-widefield optical coherence tomography to investigate relationships between myopic macular retinoschisis and posterior staphyloma. Ophthalmology. 2018;125(10):1575–86.
12. Ohno-Matsui K, Kawasaki R, Jonas JB, et al. International photographic classification and grading system for myopic maculopathy. Am J Ophthalmol. 2015;159(5):877–83.e7.
13. Cheung CMG, Ohno-Matsui K, Wong TY, et al. Influence of myopic macular degeneration severity on treatment outcomes with intravitreal aflibercept in the MYRROR study. Acta Ophthalmol. 2019;97(5):e729–35.
14. Wong YL, Sabanayagam C, Ding Y, et al. Prevalence, risk factors, and impact of myopic macular degeneration on visual impairment and functioning among adults in Singapore. Invest Ophthalmol Vis Sci. 2018;59(11):4603–13.
15. Fujiwara T, Imamura Y, Margolis R, et al. Enhanced depth imaging optical coherence tomography of the choroid in highly myopic eyes. Am J Ophthalmol. 2009;148(3):445–50.
16. Ikuno Y, Tano Y. Retinal and choroidal biometry in highly myopic eyes with spectral-domain optical coherence tomography. Invest Ophthalmol Vis Sci. 2009;50(8):3876–80.
17. Yokoi T, Jonas JB, Shimada N, et al. Peripapillary diffuse Chorioretinal atrophy in children as a sign of eventual pathologic myopia in adults. Ophthalmology. 2016;123(8):1783–7.
18. Fang Y, Du R, Nagaoka N, et al. OCT-based diagnostic criteria for different stages of myopic maculopathy. Ophthalmology. 2019;126(7):1018–32.
19. Ohno-Matsui K, Jonas JB, Spaide RF. Macular Bruch membrane holes in highly myopic patchy Chorioretinal atrophy. Am J Ophthalmol. 2016;166:22–8.
20. Ohno-Matsui K, Yoshida T, Futagami S, et al. Patchy atrophy and lacquer cracks predispose to the development of choroi-

dal neovascularisation in pathological myopia. Br J Ophthalmol. 2003;87(5):570–3.
21. Yoshida T, Ohno-Matsui K, Yasuzumi K, et al. Myopic choroidal neovascularization: a 10-year follow-up. Ophthalmology. 2003;110(7):1297–305.
22. Wolf S, Balciuniene VJ, Laganovska G, et al. RADIANCE: a randomized controlled study of ranibizumab in patients with choroidal neovascularization secondary to pathologic myopia. Ophthalmology. 2014;121(3):682–92.e2.
23. Ikuno Y, Ohno-Matsui K, Wong TY, et al. Intravitreal Aflibercept injection in patients with myopic Choroidal neovascularization: the MYRROR study. Ophthalmology. 2015;122(6):1220–7.
24. Ruiz-Moreno JM, Montero JA, Araiz J, et al. Intravitreal antivascular endothelial growth factor therapy for choroidal neovascularization secondary to pathologic myopia: six years outcome. Retina. 2015;35(12):2450–6.
25. Ohno-Matsui K, Ikuno Y, Lai TYY, Gemmy Cheung CM. Diagnosis and treatment guideline for myopic choroidal neovascularization due to pathologic myopia. Prog Retin Eye Res. 2018;63:92–106.
26. Ohno-Matsui K, Jonas JB, Spaide RF. Macular Bruch membrane holes in choroidal neovascularization-related myopic macular atrophy by swept-source optical coherence tomography. Am J Ophthalmol. 2016;162:133–9.e1.
27. Cheung CMG, Arnold JJ, Holz FG, et al. Myopic choroidal neovascularization: review, guidance, and consensus statement on management. Ophthalmology. 2017;124(11):1690–711.
28. Lai TY, Cheung CM. Myopic choroidal neovascularization: diagnosis and treatment. Retina. 2016;36(9):1614–21.
29. Takano M, Kishi S. Foveal retinoschisis and retinal detachment in severely myopic eyes with posterior staphyloma. Am J Ophthalmol. 1999;128(4):472–6.
30. Ikuno Y, Sayanagi K, Soga K, et al. Foveal anatomical status and surgical results in vitrectomy for myopic foveoschisis. Jpn J Ophthalmol. 2008;52(4):269–76.
31. Shimada N, Ohno-Matsui K, Baba T, et al. Natural course of macular retinoschisis in highly myopic eyes without macular hole or retinal detachment. Am J Ophthalmol. 2006;142(3):497–500.
32. Gaucher D, Haouchine B, Tadayoni R, et al. Long-term follow-up of high myopic foveoschisis: natural course and surgical outcome. Am J Ophthalmol. 2007;143(3):455–62.
33. Ikuno Y, Gomi F, Tano Y. Potent retinal arteriolar traction as a possible cause of myopic foveoschisis. Am J Ophthalmol. 2005;139(3):462–7.
34. Panozzo G, Mercanti A. Optical coherence tomography findings in myopic traction maculopathy. Arch Ophthalmol. 2004;122(10):1455–60.
35. Baba T, Ohno-Matsui K, Futagami S, et al. Prevalence and characteristics of foveal retinal detachment without macular hole in high myopia. Am J Ophthalmol. 2003;135(3):338–42.
36. Takahashi H, Tanaka N, Shinohara K, et al. Ultra-widefield optical coherence tomographic imaging of posterior vitreous in eyes with high myopia. Am J Ophthalmol. 2019;206:102–12.
37. Itakura H, Kishi S, Li D, et al. Vitreous changes in high myopia observed by swept-source optical coherence tomography. Invest Ophthalmol Vis Sci. 2014;55(3):1447–52.
38. Kobayashi H, Kishi S. Vitreous surgery for highly myopic eyes with foveal detachment and retinoschisis. Ophthalmology. 2003;110(9):1702–7.
39. Ikuno Y, Sayanagi K, Ohji M, et al. Vitrectomy and internal limiting membrane peeling for myopic foveoschisis. Am J Ophthalmol. 2004;137(4):719–24.
40. Shimada N, Sugamoto Y, Ogawa M, et al. Fovea-sparing internal limiting membrane peeling for myopic traction Maculopathy. Am J Ophthalmol. 2012;24:24.
41. Ho TC, Chen MS, Huang JS, et al. Foveola nonpeeling technique in internal limiting membrane peeling of myopic foveoschisis surgery. Retina. 2012;32(3):631–4.
42. Shinohara K, Shimada N, Takase H, Ohno-Matsui K. Functional and structural outcomes after fovea-sparing internal limiting membrane peeling for myopic macular retinoschisis by microperimetry. Retina. 2019; https://doi.org/10.1097/IAE.0000000000002627.
43. Gaucher D, Erginay A, Lecleire-Collet A, et al. Dome-shaped macula in eyes with myopic posterior staphyloma. Am J Ophthalmol. 2008;145(5):909–14.
44. Caillaux V, Gaucher D, Gualino V, et al. Morphologic characterization of dome-shaped macula in myopic eyes with serous macular detachment. Am J Ophthalmol. 2013;156(5):958–67.
45. Imamura Y, Iida T, Maruko I, et al. Enhanced depth imaging optical coherence tomography of the sclera in dome-shaped macula. Am J Ophthalmol. 2011;151(2):297–302.
46. Ellabban AA, Tsujikawa A, Matsumoto A, et al. Three-dimensional tomographic features of dome-shaped macula by swept-source optical coherence tomography. Am J Ophthalmol. 2013;155(2):320–8.e2
47. Fang Y, Jonas JB, Yokoi T, et al. Macular Bruch's membrane defect and dome-shaped macula in high myopia. PLoS One. 2017;12(6):e0178998.
48. Kaneko Y, Moriyama M, Hirahara S, et al. Areas of nonperfusion in peripheral retina of eyes with pathologic myopia detected by ultra-widefield fluorescein angiography. Invest Ophthalmol Vis Sci. 2014;55(3):1432–9.
49. Moriyama M, Ohno-Matsui K, Futagami S, et al. Morphology and long-term changes of choroidal vascular structure in highly myopic eyes with and without posterior staphyloma. Ophthalmology. 2007;114(9):1755–62.
50. Ishida T, Moriyama M, Tanaka Y, et al. Radial tracts emanating from Staphyloma edge in eyes with pathologic myopia. Ophthalmology. 2014;122(1):215–6.